Cement & Concrete Composites 32 (2010) 327–338

Contents lists available at ScienceDirect

Cement & Concrete Composites

journal homepage: www.elsevier.com/locate/cemconcomp

Spatially resolved evolution of adhesion properties of large porcelain tiles

A. Wetzel [a,*], R. Zurbriggen [b], M. Herwegh [a]

[a] Institute of Geological Sciences, University of Berne, Berne, Switzerland
[b] Elotex AG, Sempach Station, Lucerne, Switzerland

ARTICLE INFO

Article history:
Received 4 November 2009
Received in revised form 29 January 2010
Accepted 5 February 2010
Available online 12 February 2010

Keywords:
Polymer-modified mortar
Tile adhesive
Porcelain tile
Adhesion strength
Large-size

ABSTRACT

The rising number of failures of porcelain tiles, especially in outdoor applications, is to some extent a consequence of the critical combination of applying tiles of large dimensions and the non-porous nature of these tiles. A special setup allows a reproducible application of large-sized tiles (30 × 30 cm). In analogy to outdoor conditions, samples were stored under dry and wet conditions and have been investigated with different physico-chemical approaches. Under dry storage conditions adhesion strength is significantly lower along the periphery of the tiles compared to their centre. This reduction in adhesion performance is mainly caused by shrinkage of the mortar and substrate (~0.1 mm/m). In situ observations through glass tiles indicate that the stresses induced by shrinkage are highest in the rim regions of the tiles. Under wet storage conditions, water percolates into the rim regions of the mortar, which leads to swelling of mortar and substrate, accelerating the delamination process. The findings of this study confirm observations on the construction site, where initial failures are often found at the periphery of large-sized tiles.

1. Introduction

The number and variety of failures on tiled floors and walls increased in recent years [1,2]. Observations on the building sites reveal that initial failure (delamination) often occurs at the edges of tiles. Intrusion of water, mainly present in outdoor applications, intensifies these delamination processes [3,4]. Many of these failures can be correlated with two market trends: the application of large-sized tiles and the use of non-porous porcelain tiles. Driven by shrinkage of mortar and substrate, shear stresses at the interfaces of mortar and tile increase from centre to rim [5,6]. The larger the tiles' size, the higher the shear stresses generated by shrinkage. At the mortar–tile and mortar–substrate interfaces, the appearance of initial cracks and crack propagation is expected. These cracks are caused by differential physical response of the three layers tile-mortar–substrate to variations of external parameters (temperature, humidity, etc.) starting from early shrinkage during curing of the mortar up to daily and seasonal differential movements in the finally hardened mortar. The difference of material properties, for example in the case of the Young's modulus, is higher between tile and mortar compared to the difference between mortar and the most commonly used substrates. Therefore, the mortar–tile interface can be classified as more critical. Porcelain tiles have a high stain resistance as well as a reduced capacity for humidity-induced expansion or frost damages [7]. This is caused by their high sintering temperature and the resulting very low porosity in contrast to highly porous ceramic tiles generally sintered at lower temperatures [8]. Unfortunately, the glassy character of the porcelain tiles backside causes a reduced adhesion of the underlying mortar [9,10].

In contrast to the compressive strength of concrete, adhesion strength is the important parameter for the durability of tile adhesive mortar, while compressive strength can be neglected. The adhesion strength conventionally is tested on 5 × 5 cm large-size tiles following EN 12004. Adjusting the type or the amount of polymer increases the adhesion strength [11,12]. Former studies [13,14] investigated polymer-modified tile adhesive mortars using such small ceramic tiles. In the context of drying, comparisons between small- and large-sized tiles are critical because of pronounced differences in the drying behaviour. While small-sized tiles are drying within hours–days, which corresponds to drying of edge positions of large-sized tiles, the centre positions of the latter require months to dry. Hence, heterogeneous distributions of the mechanical properties must be expected for large-sized tiles. In order to improve the understanding of the history of material failures and to remain closely related to construction site practice, we used the previous works mentioned above to develop a suitable experimental setup. In a first step, a sample series of large-sized tiles (30 × 30 cm) were applied on a concrete substrate (40 × 40 cm) using a tile adhesive typical for floor applications.

* Corresponding author. Tel.: +41 31 631 8772; fax: +41 31 631 4843.
E-mail addresses: wetzel@geo.unibe.ch (A. Wetzel), roger.zurbriggen@akzonobel.com (R. Zurbriggen), marco.herwegh@geo.unibe.ch (M. Herweg.

0958-9465/$ - see front matter © 2010 Elsevier Ltd. All rights reserved.
doi:10.1016/j.cemconcomp.2010.02.002

The aim of this series was to compare the evolution of spatial distribution in light of: (i) mechanical properties (adhesion strength), (ii) variations in lateral dimensions due to shrinkage or expansion, (iii) lateral and vertical differences in degree of hydration and (iv) the quality of the mortar–tile interface with respect to microcracking and delamination.

A special setup was required to guarantee the reproducibility of application of large-sized tiles. As will be documented in more detail below, with the present set of experiments we push the system towards extreme conditions in terms of drying and water uptake. In this way, we can simulate working constraints, which mimic extreme climatic conditions.

Below, first the experimental setup is described followed by a presentation of the spatial variations of the mortar's physical and chemical properties for samples stored under dry and wet conditions. In a second part, these results are discussed in light of the evolution over several months and associated variations in the spatial distribution. Finally, the findings are related to the application on the building site.

2. Materials and experimental setup

2.1. Polymer modified tile adhesive mortar

Dry mortar contains hydraulic binders, mineral fillers and organic additives. In this study an ordinary Portland cement is used as hydraulic binder, quartz sand and dolomitic powder served as fillers. To keep the formulation close to applications on the construction site, but simple regarding the number of different components, only two types of polymers, unmodified cellulose ether (CE) and redispersible polymer powder (RPP), were added (Table 1).

Regardless of the low contents, the admixtures can influence the physical properties of the mortars substantially. Cellulose ether is a rheological modifier, which mainly acts as a water retaining agent, air-entraining agent and thickener. Gained by spray drying of a polymer suspension, a RPP redisperses in water and forms latex films during drying. Based on the resulting three-dimensional network of polymer films, the mortar obtains a higher flexibility and strength [11,15]. The workability of fresh mortar and the quality of the finally hardened mortar closely rely on the type and the quantity of these two additives. This mortar formulation corresponds to C2 quality after EN 12004.

2.2. Preparation of fresh mortar, substrate and tile

Add 1.2 kg of the dry mortar to 0.3 kg water and mixed with a propeller mixer (80 mm ∅, 750 rpm) in a plastic bin (16 cm ∅). The mortar is mixed for 30 s, stirred for 15 s with a hand spatula and again mixed for 30 s with the propeller mixer. The following maturing time was set to 5 min, before final stirring of the mortar for another 15 s with the hand spatula.

The concrete substrate (Antoniazzi, type RUEN) is stored for 28 days under standard conditions (23 °C/50% r.h.) before the samples are prepared. The structures on the backsides of the tiles vary due to the manufacturer and, in the case of the used tiles, differ from core to rim. Additionally, the backsides of the tiles are covered very irregularly with a white slurry previous to firing to avoid sticking on the band-conveyor of the kiln [10]. Thus, the backsides of the tiles were abraded by a grinding machine (manufactured by Wenzler) with a diamond cup wheel cooled by water. By abrading these structures, the surface becomes homogeneously flat over the entire backside.

Table 1
Dry mix composition of flow-bed mortar for floor applications.

Dry mix	wt.%
CEM I 52.5 R	35.0
Quartz sand 0.1–0.6 mm	15.0
Quartz sand 0.1–0.3 mm	31.6
Dolomite powder	15.0
Unmodified CE	0.4
Redispersible polymer powder	3.0
Water	25.0

Table 2
Difference in degree of hydration at certain positions, heights and storage conditions are given in percent.

Differences	(%)
Upper and lower layer (core dry)	**12.8**
Upper and lower layer (rim dry)	6.4
Upper and lower layer (core wet)	2.5
Upper and lower layer (rim wet)	5.8
Wet–dry (core position)	8.2
Wet–dry (rim position)	**15.5**
Core-rim (dry)	**10.2**
Core-rim (wet)	2.6

2.3. Setup of application gauge

To guarantee the reproducibility of samples consisting of 30 × 30 cm large tiles, an application gauge was developed. In this way, the position of the tile in respect to the mortar ribs and grooves as well as centric positioning of all materials (tile, mortar, and concrete substrate) ensures the production of symmetrical samples (Fig. 1). For documentation a digital camera was mounted on a fixed tripod on top of the gauge.

The concrete substrate (a) is placed on the application gauge (Fig. 1). Afterwards, the outermost 4 cm were covered by an ordinary adhesive tape (b), allowing a defined area in the substrate's centre to be covered by mortar. The latter is of particular importance in light of later drying (see below). After these preparative steps, the fresh mortar is mixed following the above-mentioned procedure. A thin contact layer of fresh mortar is applied with a hand spatula (c). Subsequently the remaining mortar is applied on the contact layer. Using a notched flow-bed trowel (type M1, 7.3/12/20), the mortar is combed three times. Thereby the trowel is guided on a catch (Fig. 1, see point 2) holding a constant angle of 60° between trowel and substrate. As a consequence of this geometrical setup, the later inlayed tile ends up in a middle of a rib on the right- and left-hand side. An adjustment frame is fixed on the main application gauge (Fig. 1, see point 3) to ensure a central positioning of the tile (d). Without lateral movements (no shearing) a

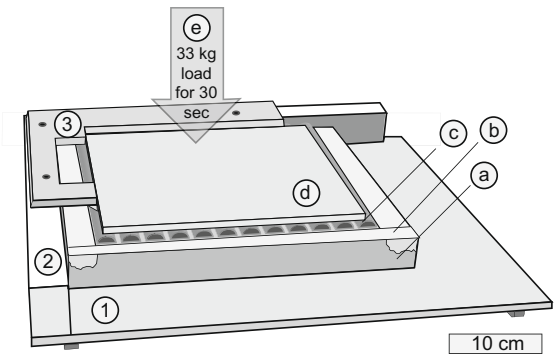

Fig. 1. Setup of application gauge consisting of three parts: ground plate (1), side frame (2), and tile adjustment frame (3). Steps a to e are described in detail in the main text.

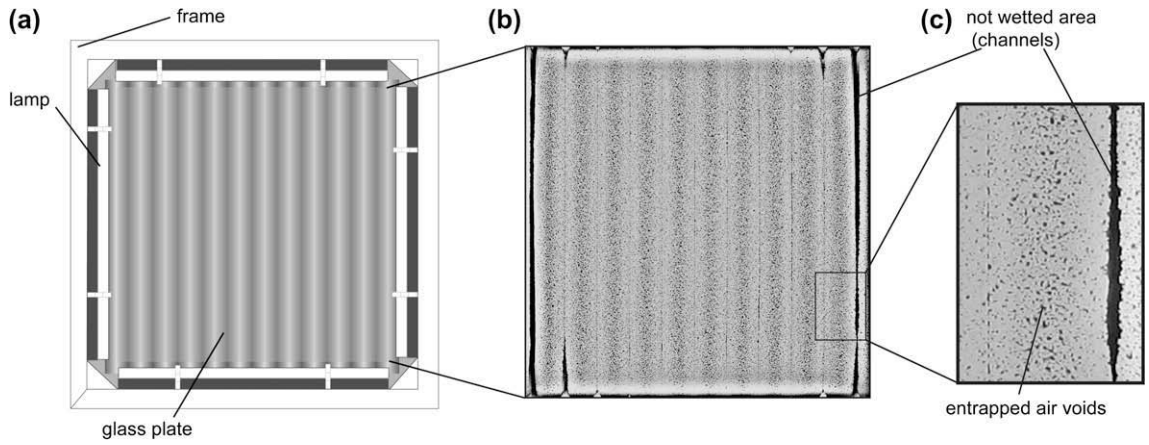

Fig. 2. (a) Setup (top-view) of light-frame as used for investigations of the interface between mortar and glass tile. The stripes seen through the glass-plate correspond to the trowel pattern (ribs and grooves). (b) The mortar–glass interface 1 week after application with close-up view (c).

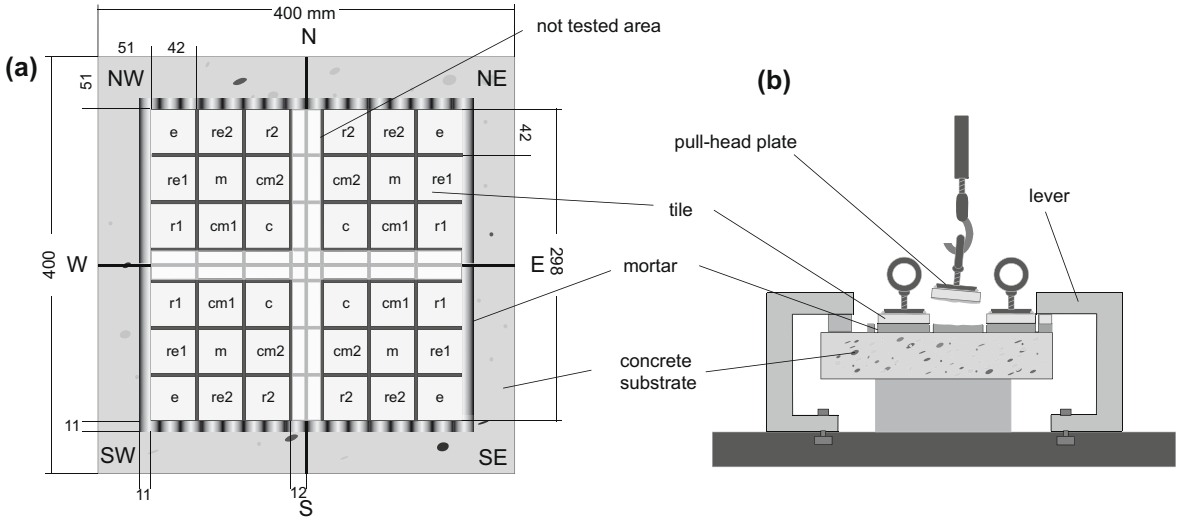

Fig. 3. (a) Top-view sketch of the cutting pattern. First, the sample is cut along N–S and E–W into four equally dimensioned quadrants. Second, the tile and mortar bed of each quadrant is cut into nine mosaics (each measuring 42 × 42 mm), which individually are subjected to a pull-out test (b).

vertical load (33 kg) is placed on top of the tile for 30 s (e). After the adjustment frame and the adhesive tape are replace, the sample is directly stored under standard conditions (23 °C/50% r.h.).

2.4. Experimental series

Following the described procedure, several samples were prepared for: (i) spatially resolved adhesion strength tests, (ii) investigations on the mortar–tile interface, (iii) measurements of variations of lateral dimensions, (iv) estimations of drying rates and (v) thermogravimetric analyses for estimation of the degree of hydration. At periodic time intervals these investigations were carried out over a total of four months. A complete experimental series consists of nine samples for adhesion strength tests, a glass plate sample for interface investigations and one sample for the measurement of dimensional variations. To compare different storage conditions, two sample series were produced and stored under dry (23 °C/50% r.h.) and wet (1 week at 23 °C/50% r.h., followed by water storage) conditions, respectively.

The setup of sample preparation simulates an extreme situation. No grouts were applied so that the mortar can directly interact with exterior influences (air for dry storage, water for wet storage).

2.5. Light-frame setup

For the purpose of continuous in situ observations of the structures (such as wetting pattern, entrapped air voids, cracks) at the mortar–tile interface, each series contains a special sample, which is prepared with a transparent glass plate (ordinary window glass) with identical dimensions (30 × 30 × 0.8 cm) like the porcelain tiles. But, it must be kept in mind that the two materials (ceramic tile versus float glass) differ in roughness and water uptake capacity. A fully vitrified ceramic tile has a water uptake of less than 0.5 wt.% according to EN 14411, while glass takes up no water at all. SEM investigations indicate that the tile's roughness is higher compared to the even and smooth glass. The structure of the mortar is built up by ribs and grooves resulting from the notched trowel. The ribs are pressed down by vertical pressure, while inlaying of the tile and the grooves are filled with mortar from the sheared ribs. On the left- and right-hand side of the tile, the grooves are not completely filled and along these grooves channels remain, which

are oriented parallel to the ribs. Along these channels, the tile is not wetted by the mortar.

To achieve a complete and homogeneous illumination of the entire interface (30 × 30 cm), a light-frame (Fig. 2a) was developed. Both dry and wet stored samples were documented by photographs at periodic time intervals from a top-view (Fig. 2b).

2.6. Setup for adhesion strength tests

The spatial variation in adhesion strength over the area of a 30 × 30 cm sized tile can be gained by separating the area into mosaic parts (Fig. 3) and testing each of them individually by a pull-out test.

The following preparation steps are required prior to testing. One day before the pull-out tests, pull head plates (40 mm ∅) are fixed by a two-component adhesive on the pre-defined positions of the mosaics. Due to spatial restrictions of the pull-out device, the sample has then to be cut in four equivalent quadrants. On the inside faces of the quadrants strips of approximately 12 mm are left over as levers for the pull-out machine (Fig. 3a). Subsequently, on each quadrant notches are cut through the tile and mortar layer under dry conditions using a table saw equipped with a diamond blade. Each part of the resulting mosaic measures 42 × 42 mm. Subsequent to these cutting procedures, the pull-out tests are carried out. The mosaics are labelled systematically according to their positions. Labels *e*, *m*, *c* and *r* refer to positions at the edge, middle, centre and rim of the tile, respectively. Positions in between have a combined code, e.g., *cm1* (Fig. 3a). Each of the nine mosaic positions is unique with respect to the distance from rim and the wetting pattern. Pull-out tests were performed following EN 12004 and failure modes were classified according to EN ISO 10365.

2.7. Setup for measurements of dimensional variations

In the scope of this project, special attention is paid to the question of how the different materials shrink and expand relative to each other (differential strain). In order to measure the shrinkage on a "real" system (restrained shrinkage), plug gauges are fixed on the surface of the tile and on top of the concrete substrate as shown in Fig. 4. Before inlaying of the tile, the distances between the plugs are measured to gain an initial value. After application the distances are measured at periodic time intervals by a digital micrometer (Fig. 4a).

2.8. Sampling for thermogravimetric analysis

In order to resolve hydration gradients (by thermogravimetric analysis) as a function of location and time, sampling was carried out at specific sites (Fig. 5).

Mortars from the remaining strips, used as a lever for the adhesion strength tests, were locally sampled for thermogravimetric analyses (TGA). After the tile was removed, mortar material was collected at five different vertical positions in the mortar layer with a hand spatula following a method developed by De Gasparo [16]. After the samples were dried for one day at 40 °C, about 100 mg per sample were tested under air flow (50 ml/min) between 30 °C and 1000 °C, with a heating rate of 10 °C/min.

3. Results

3.1. Distribution of adhesion strength

After the adhesion strength tests were carried out (Section 2.5), the surfaces of the bottom of the mosaic parts were documented under light gleaming from the sides. The wetting of the tile by

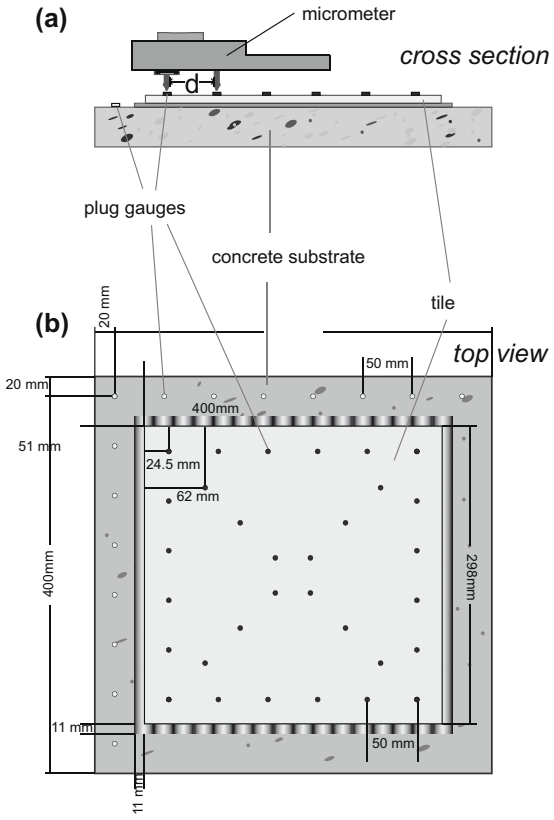

Fig. 4. Experimental setup for the measurements of variations in the lateral dimensions, (a) in side-view and (b) in top-view. Plug gauges were fixed on the surface of tile and concrete substrate with a spacing *d* of 5 cm.

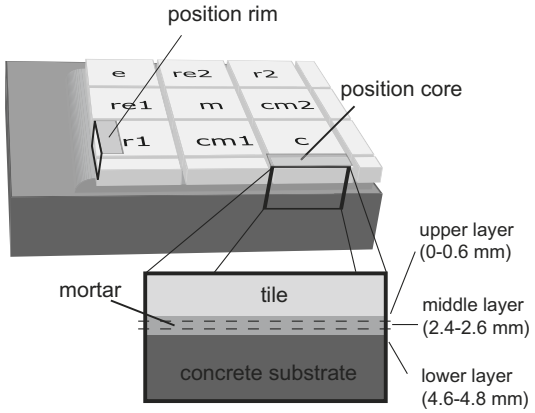

Fig. 5. For thermogravimetric analyses, at positions in the core and at the rim the mortar was sampled at three different vertical locations, near the tile, in the middle of the mortar bed, and near the substrate.

the mortar can be seen very clearly in that way and can be compared to the pattern seen in the glass plate experiments. At the rims parallel to the trowelling direction, the wetted area is lowest (Fig. 6). Along the interspaces between former ribs, cohesion failures can be noticed, which clearly indicate enhanced adhesion strength at the interface compared to the cohesion strength of the mortar's interior. Because this is only one of some influencing variables affecting a distribution of adhesion strength, it will be discussed later.

Fig. 7 shows the distribution maps of adhesion strength of the entire tiles (30 × 30 cm). Areas of untested stripes (see Fig. 6) were

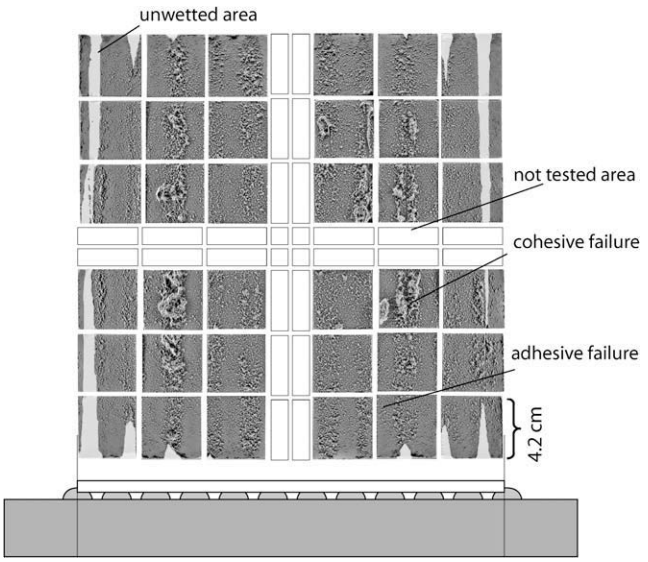

Fig. 6. The backsides of mosaic parts after pull-out test of the sample stored 4 weeks under dry conditions (23 °C/50% r.h.). For comparison a schematic cross section of tile, mortar (rib geometry) and substrate is shown below.

interpolated from values of adjacent mosaic positions. Within a single tile, the four quadrants show comparable results indicating a good reproducibility regarding the experimental procedure. Lowest values occur at the rims on the right- and left-hand sides (corresponding to the positions *e*, *re1*, *r1*, Fig. 3). In between core and rim, especially at the positions *m* and *cm1*, generally the highest values appear. Until the 8th week, the mentioned distribution remains, but the adhesion strength increases, inducing an increasing difference between the low and high strength domain (Figs. 7 and 8). Afterwards, the adhesion strength slightly decreases.

The wet stored samples show lower values and reduced differences in adhesion strength compared to the dry stored ones (Figs. 7 and 8). Although the values are smallest at the left- and right-hand rim, which correlates with the dry stored samples, only a very low maximum for the values at the positions *m* and *cm1* can be observed.

Fig. 8 shows the evolution of adhesion strengths averaged over the equivalent positions on the four quadrants. Position *e* at the edge reaches a plateau already after 1 week. The positions *re1* and *r1* show quite similar evolution, though the values are higher than at the edge and the variations in amplitudes are more pronounced. The positions *e*, *re1*, *r1* (group *A*) are influenced by an incomplete wetting and early drying due to their peripheral locations. Positions *re2* and *r2* (group *B*) have the same distance to the rim and therefore are also drying quickly, but are affected only weakly by incomplete wetting. In contrast, positions *m*, *cm*1, *cm2*, *c* (group *C*) are completely wetted and are drying slowly. They reflect the highest adhesion strengths. Adhesion is significantly lower under wet conditions (Fig. 8b). Positions *e*, *re1*, *r1* show considerable variations in adhesion strength, while the values of the other positions lie closely together. Except for a subordinate culmination after 8 weeks, the values constantly increase until the 18th week.

Fig. 9 focuses on the spatial differences in failure pattern in the context of dry and wet storage as well as their evolution. Illustrated are the NW-quadrants of the samples tested after 2, 8 and 18 weeks of dry and wet storage, respectively. Because the whole experimental setup represents a vertical and horizontal mirror symmetry, it is sufficient to focus on a single quadrant only. The schematic sketch on cohesion/adhesion failure (Fig. 9h) shows the change in the failure pattern in dependence of both the former rib and groove positions, as well as the runtime of the experiment.

The correlation between failure pattern and former groove and rib geometries is quite strong in the case of dry stored samples (Figs. 9a–c). Similar to the experiments of Jenni et al. [17] adhesion failure in large-sized tiles generally occurs at the interface between former ribs and tile. In contrast, cohesion failure mainly occurs at former grooves, i.e., locations in which the wet mortar has been sheared in during inlaying of the tile (Fig. 10). In terms of the temporal evolution, the percentage of adhesion failure remains nearly constant during the first 4 weeks but decreases afterwards. In contrast, cohesion failure occurs at maximum depth in the mortar bed

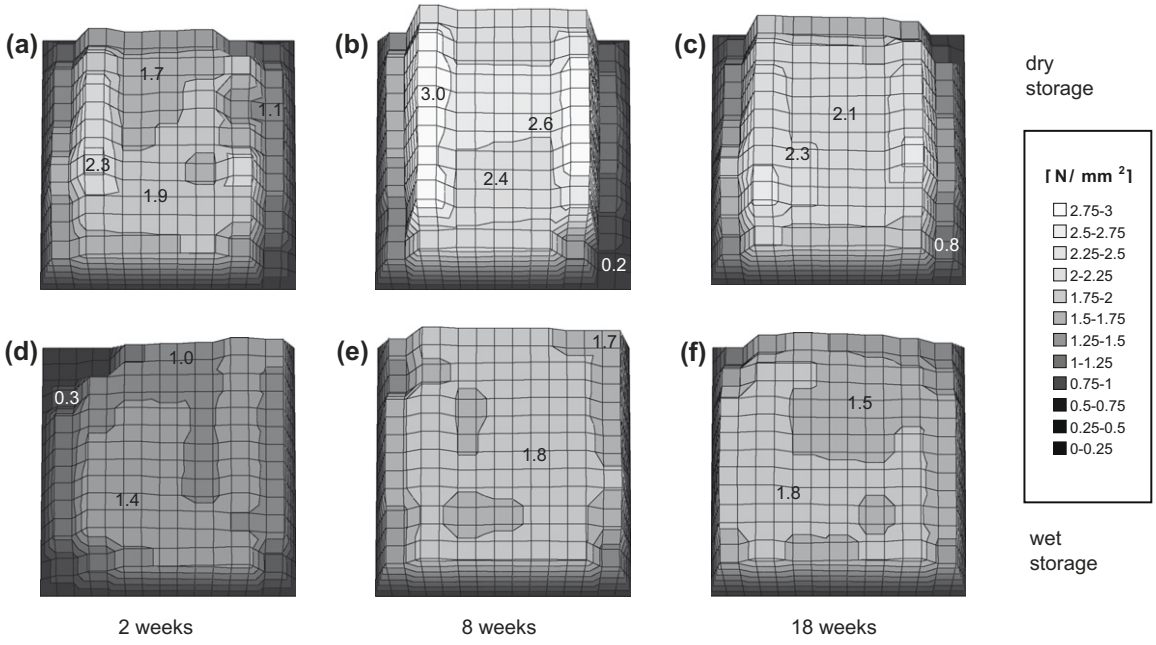

Fig. 7. Distribution maps of adhesion strength under porcelain tiles (30 × 30 cm) after (a) 2 weeks, (b) 8 weeks and (c) 18 weeks of dry storage and wet storage (d–f). The Distribution maps are based on strength data obtained by pull-out tests carried out over 36 individual mosaics covering the entire tile surface and are illustrated in a surface plot (Microsoft Excel).

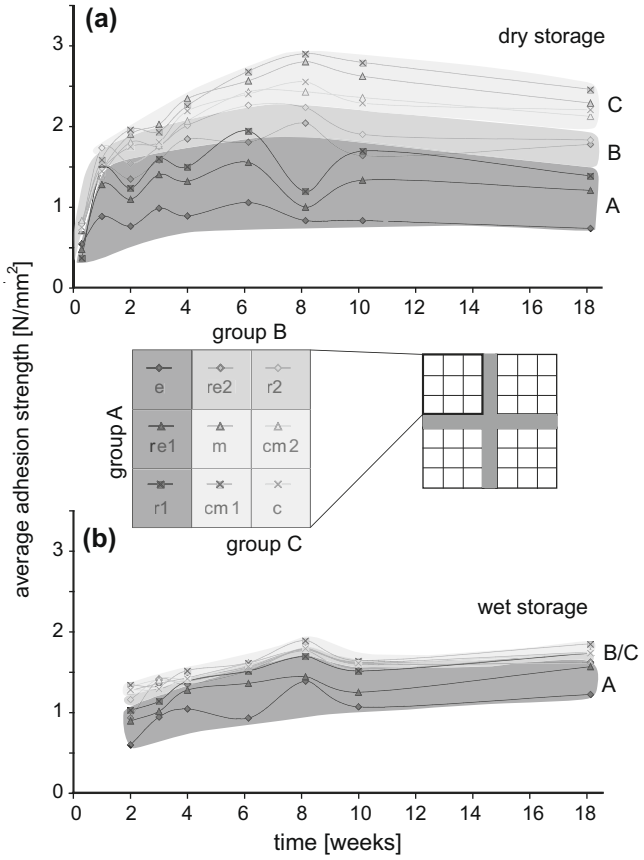

Fig. 8. The average values of adhesion strength at given positions are plotted as a function of runtime for (a) dry storage and (b) wet storage.

in the 2nd week, lasting at this level until the 4th week but rises into shallower levels afterwards (Fig. 9h). According to ISO 10365 the final fracture patterns of the whole sample can be described as an intermediary state between cohesion failure and special cohesion failure.

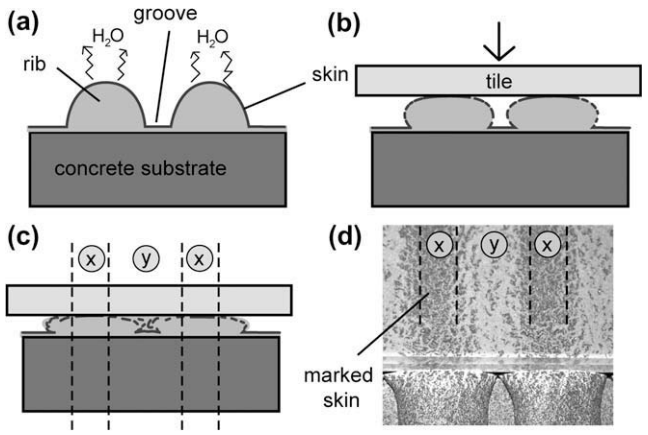

Fig. 10. (a–c) Deformation of fresh mortar including skin at the surface during tile application. (d) Top-view of an applied glass plate; the skin of the mortar was marked by an ordinary spray paint.

The wet samples show a different evolution in failure modes (Figs. 9d–f). Right from the start of wet storage, the locations of cohesion failure occur at shallow levels in the mortar bed resulting in an almost planar fracture surface after 18 weeks. Hence, the differences in height between cohesion fractures at rib and groove locations are smaller compared to dry storage (Fig. 9h). Summing up, dry stored samples change the failure pattern from adhesion/cohesion failure to special cohesion/cohesion failure, while wet samples change from special cohesion/cohesion failure to cohesion failure (ISO 10365).

3.2. Interface investigations

Transparent glass plates, applied instead of tiles (Section 2.4.), allow in situ observations of the development of structures at the tile-mortar interface such as: (i) local wetting percentage, (ii) air entrapment, (iii) shrinkage cracks (during dry storage) and (iv) water front (during wet storage).

Directly after application of the fresh mortar up to the moment the tile is laid in, the uppermost layer of the mortar is interacting

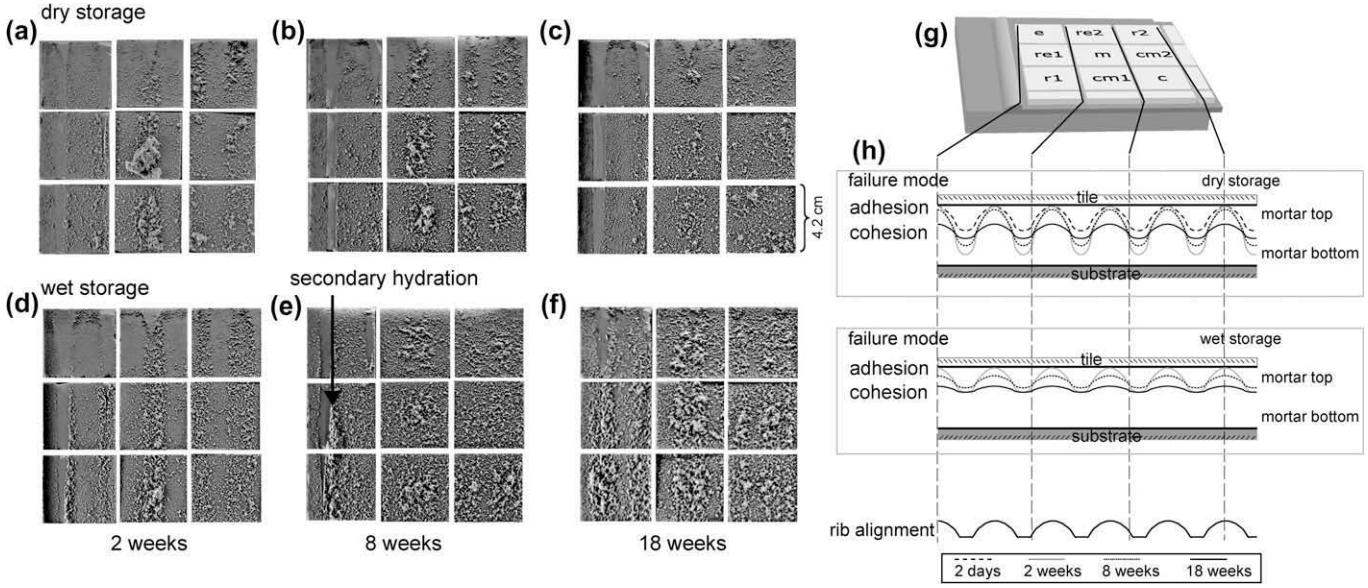

Fig. 9. Backsides of the mosaic parts (NW-quadrants) with evolving failure pattern under dry (a–c) and wet (d–f) storage conditions. (g) A 3-D-sketch shows the NW-quadrant with the mosaic positions tested for the adhesion strength. (h) The dependency of rib alignment and mode and depth of failure surface in the mortar bed is shown schematically.

with the air. Jenni et al. [17] and De Gasparo et al. [18] demonstrated that evaporation at the air-mortar interface induces an accumulation of soluble polymers and fines. With ongoing drying a skin evolves. The thickness, composition and property of the skin depends on temperature, humidity and the time until inlaying [19]. When the tile is inlaid, the ribs are deformed by the applied pressure (Fig. 10). The skin on the top of the ribs is pressed downwards and only slightly sheared. Thus, the contact to the tile at these positions is mainly build up by skin (former rib positions). The grooves are filled by the fresh mortar, which is pressed out of the sheared ribs (Fig. 10c). Thus, the contact to the tile is built up by the fresh mortar at these locations (former groove positions). This process is confirmed by marking the skin with an ordinary spray paint directly before inlaying of a transparent glass plate (Fig. 10d).

At the rims on the right and left side of the glass plate the wetting is incomplete, while it is complete towards the centre (100% area). During inlaying of the glass plate, air is entrapped at the interface. These entrapped air voids are stable over the entire period of investigations (Fig. 2c, see also Figs. 11a1 and b1).

Besides these initial structures arising from inlaying of the tile, two types of delamination at the mortar–tile interface can be observed, which evolve during: (i) dry and (ii) wet curing. (i) Under dry storage conditions, delaminations type I (Fig. 11b1), owing to ongoing drying shrinkage, can be observed after about 6 weeks. At this time, these delaminations are only a few mm in diameter and build out elongated hypocycloids with varying numbers of cusps. With continuing drying more delamination sites nucleate; they grow and begin to coalesce forming a continuous belt along the rim of the glass plate (Fig. 11b). In addition, similar delamina-

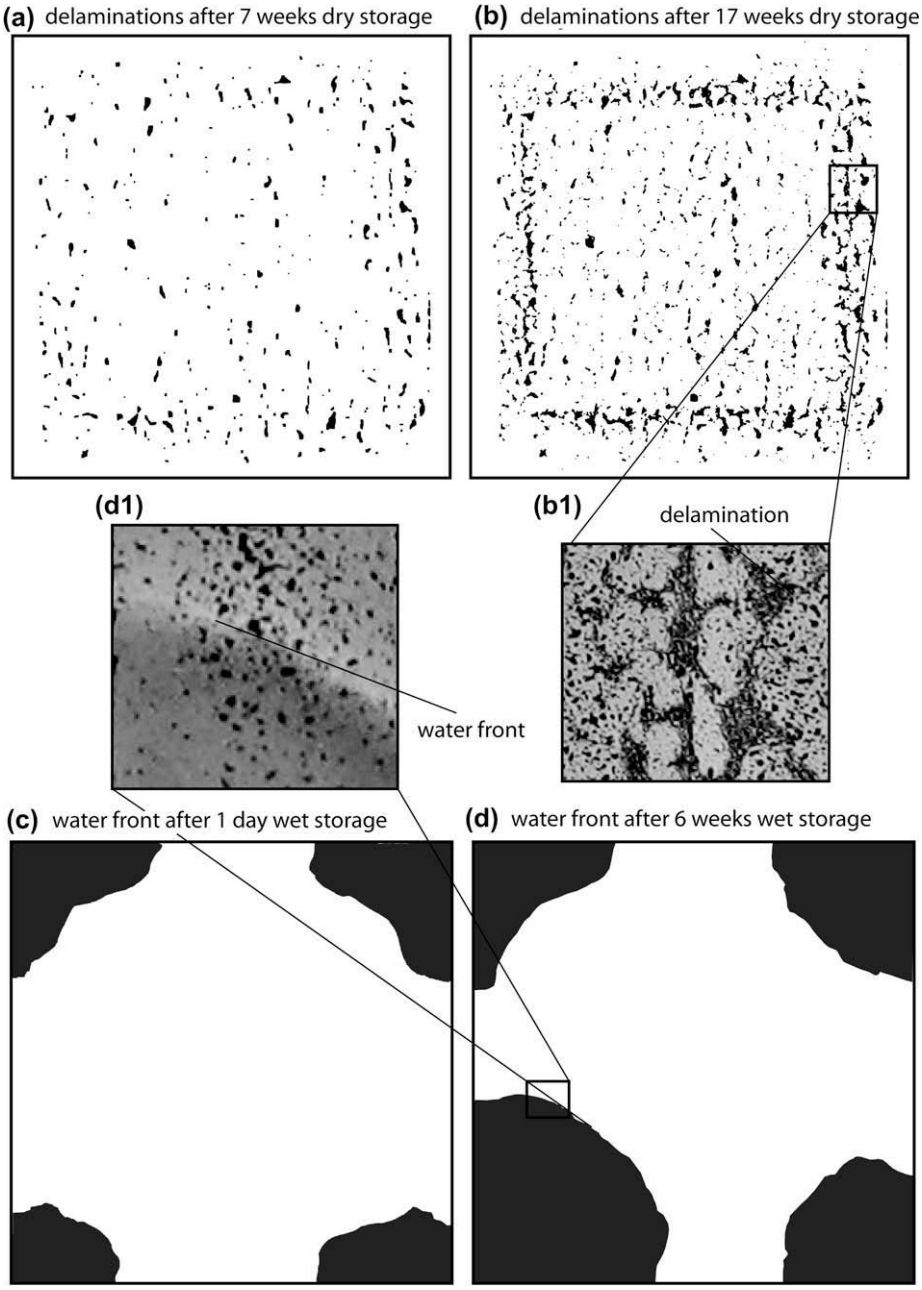

Fig. 11. Type I delaminations (black) after (a) 7 weeks and (b) after 17 weeks dry storage. (b1) Detail of type I delaminations. Type II delaminations related to water immersion after (c) 1 day and (d) 6 weeks of wet storage. (d1) Type II delaminations in detail.

tion structures occur parallel to the trowelling direction. (ii) Type II delaminations evolve over large areas at the tile-mortar interface at the edges of the glass plate after one day of water immersion (Fig. 11c). The interface volume affected by delamination serves as a water pathway and is fully filled with the latter. Over this pathway, water percolates into the mortar. This delamination front shows no significant change during the following 5 weeks. In the 7th week (after 6 weeks of water storage), however, the delamination front migrates fast towards the centre. After 8 weeks, the glass plate is completely detached.

3.3. Hydration gradient measured by thermogravimetric analysis

The degree of cement hydration was measured by thermogravimetry (weight loss from 30 to 150 °C). In general, the weight loss until 150 °C can be caused by the dehydration of primary calcium sulfates, ettringite, monosulfate and C–S–H. The reaction of primary calcium sulfates to ettringite occurs very early in the hydration sequence and can be assumed to have been completed, even at position *e*, where drying happens quite early. Thus, the variations in the weight loss can be attributed to variations in C–S–H, which is confirmed by the dehydration step of Portlandite at about 450 °C.

The relative differences regarding position (core, rim), height (upper, middle and lower layer) and storage conditions (dry, wet) are shown for the curing time of 4 weeks (Fig. 12, Table 2). As mentioned in the introduction, the amount of hydrates has a great impact on the strength of the mortar.

The degree of hydration is ~15% higher in the case of water storage compared to dry stored samples. From core to rim, the degree of hydration reduces by about 10% and less than 5% for dry and wet stored samples, respectively. The differences between core and rim is supposed to be a consequence of drying front evolution, this point will be picked up again in the discussions. The degree of hydration at the position in the middle (position *m*, Fig. 3a) showed values close to those measured in the core (position *c*). This could be shown in preliminary tests.

The vertical variation in degree of hydration is small in the case of the wet stored sample, but higher after dry storage. At the core position, a slight increase from lower to upper layer can be seen for the dry stored sample (~10%). This might be explained by a vertical pore water gradient driven by water uptake of the concrete substrate. At the rim, this effect is weaker due to the fact that drying also occurs from the side.

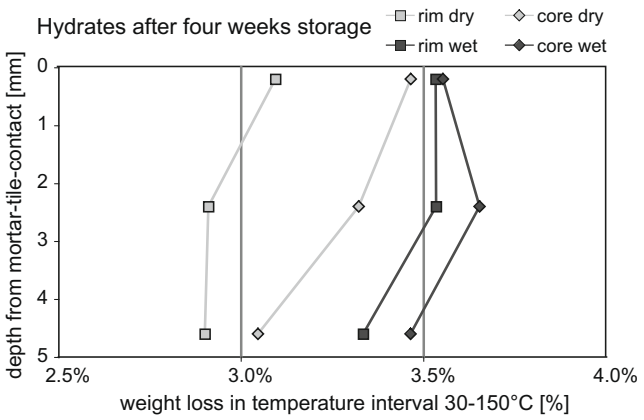

Fig. 12. Thermogravimetric analysis of hardened mortar at core and rim positions at different heights in the mortar bed (see also Table 2).

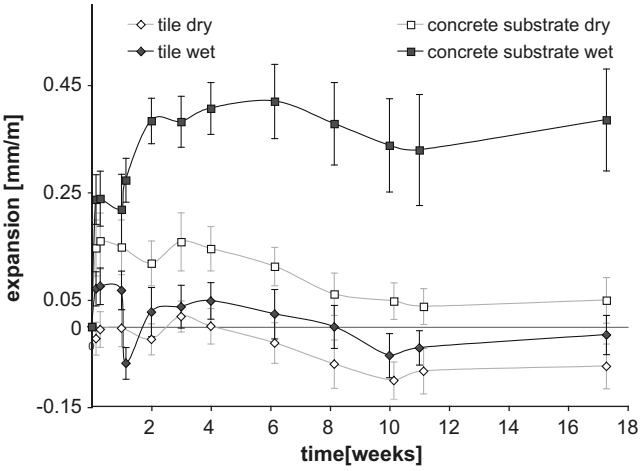

Fig. 13. Dimensional variation of tile and concrete substrate for wet and dry storage (standard deviation). Each value represents the average of at least 14 measurements.

3.4. Dimensional variations

By measuring pre-defined distances between plug gauges on the surface of the concrete substrate and ceramic tile, expansion or shrinkage can be observed (Section 2.6). The measured values did not vary strongly on either surface. Therefore, the average values of all measured distances were calculated and plotted in Fig. 13.

Under both storage conditions, the substrate always shows a higher dimensional variation compared to the tile. The differences between tile and concrete are about three times higher for the wet storage conditions. In general, expansion/shrinkage of the tile goes hand in hand with the dimensional variations in the concrete substrate.

First expansion is related to water uptake of the concrete substrate from the fresh mortar (can be seen in both samples). While no significant change can be seen for the dry stored sample until the 6th week, the sample stored under wet conditions shows clear reaction due to water immersion. One day after water immersion, the concrete substrate again shows expansion, while the tile is compressed. This indicates dishing of the sample caused by swelling of the concrete substrate. A second experiment, in which additional plug gauges were fixed on the bottom of the substrate, confirmed this explanation [20]. During the 1st week of water immersion, the compression of the tile relaxes.

After about 6 weeks, the concrete substrate and the tile show significant shrinkage for the dry stored sample and a slightly reduced shrinkage in the case of the wet stored one. From the 10th week on, the values stabilize.

4. Discussion

4.1. Temporal evolution

The temporal evolution of: (i) delaminations at the interface of glass plate and mortar, (ii) expansion/shrinkage of concrete substrate and tile, (iii) adhesion strength, and (iv) the weight loss due to drying is shown in Fig. 14. Dry and wet storage are compared for (i)–(iii).

Depending on storage conditions, two types of delaminations could be observed in the glass plate experiments. The area fraction of delaminations is illustrated in Figs. 14a and e (note the different scale of the *y*-axes). Both delaminations types (Section 3.2) result from cracks at the interface, but the driving forces leading to these delaminations are different. Type I delaminations (dry storage) are caused by shrinkage due to drying and hydration. The wet stored

sample, on the contrary, shows delamination (type II) at the edges, with more than 20% area fraction after only one day of water immersion. The mortar is locally wetted along the delaminated areas. After 8 weeks, total adhesion failure between the glass plate and mortar occurred. The processes responsible for type II are related to a combination of differential swelling and water intrusion. Local swelling driven by water uptake at the rims of the substrate leads to a dishing of the whole sample assembly. This dishing results in a rise in stress at the tile-mortar interface and stress concentrations at the edges leading to micro-crack formation at the edges. Along these cracks water intrudes, inducing local swelling of the mortar's fracture surfaces newly accessible for water. With progressing time, the delamination front therefore migrates from the edge locations towards the sample's centre.

In general, the observed structures on the glass tile sample are presumed to occur as well at the interface of mortar and porcelain tile. In light of a comparison in delamination behaviour between tile and glass plate, differences have to be expected particularly in the case of wet storage. This is corroborated by the fact that no total failure has occurred for ceramic tiles during the whole runtime of water storage. The backside of the tile is rougher than the one of the glass plate. Propagation of initial cracks is hampered by this topography preventing a complete adhesion failure as observed for the glass plates. We speculate that a reduced fracture interconnectivity reduces the infiltration of the water retarding the delamination process.

In terms of the temporal evolution of dimensional variations, the first expansion of the substrate occurred directly after application (Figs. 14b and f), which does not affect the mechanical stability of the interface, because the mortar is still plastic. Particularly the water immersion leads to a pronounced expansion of the substrate inducing the aforementioned delamination type II. Apart from that, no significant dimensional changes can be observed until the 6th week under both storage conditions. The adhesion strength is constantly increasing during this time interval (Figs. 14c and g). Between the 6th and 10th week, constant and significant shrinkage of dry and wet stored samples occur. In both cases this might be related to chemical shrinkage. In the case of the dry stored sample, the process of drying leads to shrinkage of mortar. Additionally, also the substrate looses its water, which was previously taken up from the fresh mortar directly after application. The concrete substrate and the mortar of the wet stored sample, on the contrary, are still/again water saturated and a release of water owing to evaporation is impossible. Despite the higher initial expansion of the wet stored sample, the relative amounts of shrinkage between the 6th and 10th week are similar for dry and wet storage. These shrinkage periods are associated with a strong increase in delaminations, which were observed in the glass plate samples (Figs. 14a and e). The delaminations of type II occurred first directly after water immersion, but no further delamination was observed until the 7th week. As manifested by a renewed onset of delamination, it is supposed that due to rising

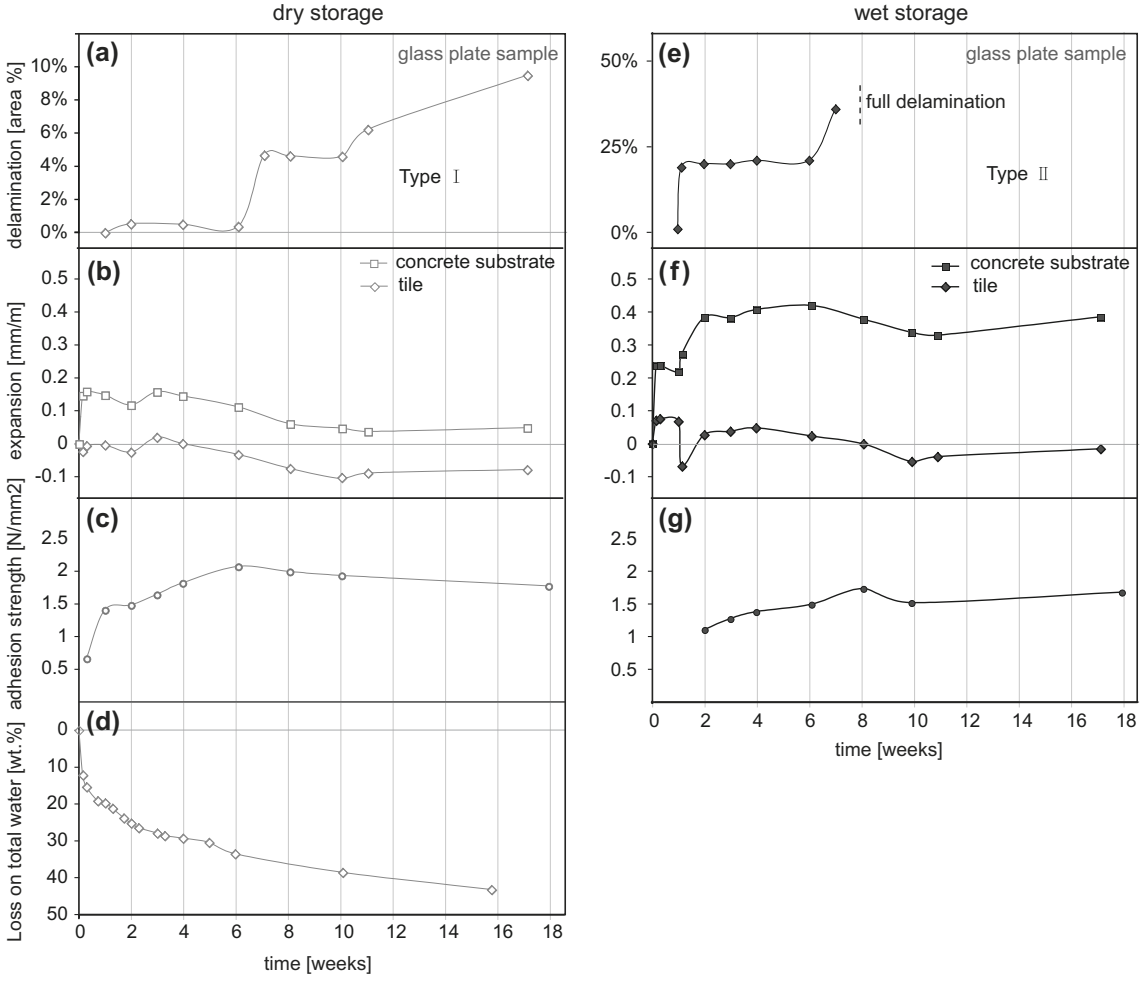

Fig. 14. Temporal evolutions of (a) the area fraction of delamination due to shrinkage, (b) expansion of concrete substrate and tile, (c) the adhesion strength averaged over all positions and d) the loss of water due to drying are illustrated for dry storage on the left side and for wet storage (e, f, and g).

hydration shrinkage, the pre-existing cracks reactivate. Further water intrusion accelerates the process again resulting even in a complete failure after 8 weeks. This failure behaviour can be explained in terms of the stress evolution at the tile-mortar interface. Owing to differential expansion/shrinkage properties of mortar and the substrate in comparison to the stiff ceramic tile, differential stresses at the tile-mortar interface will build up. At the moment these stresses cannot be accommodated by the elastic, and partly plastic, behaviour of the mortar, failure in the form of micro-cracking occurs at the interface. In addition, an increase in embrittlement is expected due to hardening of the mortar during dry and wet storage. This hardening reinforces the development of initial cracks at the interface.

Although adhesion strength was investigated in terms of spatial resolution, we will first discuss the overall evolution in adhesion strength by averaging all measurements taken at a given time interval (Figs. 14c and g). The wet stored samples show a constant increase in adhesion strength, indicating that the degree of hydration is still rising due to the availability of water. The apparent decrease in adhesion strength after 8 weeks is interpreted to result from data scatter and is probably not related to a specific process. More experiments would be needed to be conclusive to this respect. In contrast to the wet stored samples, the adhesion strengths of dry stored samples rise only until the 6th week, afterwards the values decrease. Due to hydration and drying induced loss of water, shrinkage leads to critical shear stresses. Subsequently micro-cracks evolve, which promote a decrease in adhesion strength and may even result in delaminations, as observed in the glass plate experiments (see above).

4.2. Spatial heterogeneity of mechanical properties

The adhesion strength is one of the most important aspects to evaluate the performance of a tile adhesive mortar. As we have seen throughout this study, there is a considerable number of influencing parameters. Regarding the evolution of damage on large-sized tiles, it should be kept in mind that the influences are different in respect to the position (rim or core). In light of potential damage, the designed experimental setup represents a critical end member situation. Because of lacking grouts, fast interactions between mortar and surrounding environment are promoted enabling fast drying (dry storage) or water uptake (wet storage). In Fig. 15, three positions of the tile (dry and wet stored) are compared with respect to: (a) adhesion strength, (b) fracture pattern, (c) trowelling pattern and (d) hydration gradient. The parameters which influence adhesion strength are: (i) the trowelling pattern/distribution of skin, (ii) the wetting pattern, (iii) the degree of hydration and the strengthening of polymer films, as well as (iv) the shrinkage induced shear stresses. In the following these influences on the adhesion strength will be discussed.

4.2.1. Wetting pattern

The area percentage of the wetting of the tile by the mortar is crucial for the resulting adhesion strength. During inlaying of the tile, the mortar near the rim of the tile can escape into the grout. Hence, there is less compaction resulting in the preservation of a higher amount of channels of initial trowelling. Group *A* positions (Fig. 8) show incomplete wetting, which reduces adhesion strengths. This group is represented by the position *e*, which is shown in Fig. 15.

4.2.2. Trowelling pattern/distribution of skin

Cohesion failure within former grooves indicates a stronger adhesion at the tile-mortar interface (Figs. 6 and 9). The correlation between failure pattern and trowelling pattern can be explained in the following manner. Before the tile is laid in, the mortar is exposed to the air and a skin is forming on its surface. The skin is dryer than the fresh mortar underneath and certain substances might be enriched in it [17,21]. As presented in Fig. 10, the explained pattern of different contact zones depends on the trowelling pattern, which correlates with the failure patterns (Figs. 15b and c). Along the grooves fresh mortar is pressed out of the ribs and properly wets the tile. This results in a good adhesion and failure occurs in the mortar (cohesion failure). In contrast, the still connected skin at the former rib positions, however, reflects the mechanically weakest domains during adhesion testing as manifest by location of failure at these sites (Figs. 15b and c).

4.2.3. Degree of hydration and strengthening of polymer film

Even after 18 weeks the whole system is losing weight due to evaporation of residual water (Fig. 14d). This indicates that cement hydration and polymer film strengthening still continue. Water can be lost in both lateral and vertical directions, respectively, owing to drying and soaking underground. The latter is supposed to be homogeneous over the entire area, while the effect of evaporation is enhanced in the periphery.

Formation of polymer films is related to drying and diffusion and can be classified into three stages: (i) coagulation, (ii) deformation, and (iii) coalescence [22]. Fast drying accelerates latex particle deformation by dry sintering but decelerates the coalescence of latex particles, which depends on the rate of diffusion of polymers. Hence, the strength of a polymer film depends on the complete succession of all stages as well as on the duration of the individual stages. The first two stages are reversible and the formed film can redisperse when rewetted [23]. A maximum strength of polymer films will be reached, if all three stages are passed through under ideal conditions. In this context, Jenni et al. [15] have shown that polymer films derived during slow but long formation have higher strengths.

As mentioned above, the drying of the mortar is strongly position dependent. The edge (position *e*) will be affected first by drying, afterwards position *m* and in the end position *c*. The degree of hydration therefore shows a gradient from *e* to *c*, where the hydration of $e < m \approx c$, as demonstrated by thermogravimetric analysis (Fig. 15d). The latex films along the periphery might have a reduced strength compared to central parts, because the drying front passes the rim regions too fast, preventing an ideal sequence for film formation as mentioned above. Group *A*, especially position *e*, is affected by incomplete wetting and therefore the mortar is drying out faster along the channels. Furthermore, early drying of the mortar at the periphery of the tile, especially at the edge position (*e*), can occur before or during hydraulic setting of the mortar. This early drying causes a low degree of hydration provoking enhanced shrinkage because: (i) the loss in capillary water is much higher when drying occurs early and (ii) the strength is low as well. These inferences are corroborated by the low adhesion strengths at the periphery (group *A*, Fig. 8) reaching almost maximum values already after 1 week (Fig. 8).

The wet stored samples, on the contrary, show a constant increase in adhesion strength at the edge positions (*e*). In this case, potential water loss in consequence of evaporation during 1 week of drying (see Section 2.3) is compensated by water intrusion during wet storage. This water further promotes the hydration process in the rim regions. Moreover, also more internal regions are affected by secondary hydration because of water intruding along the channels. At these positions the cohesion failure patterns affirm enhanced strengths, which might be related to the effect of reactivated hydration during water storage (Fig. 15b). After 8 weeks, the adhesion strengths at the edge positions (*e*) are higher for the wet than for the dry stored sample (Fig. 15a). On the average, however, the strengths are lower for the wet stored sample, which can be explained by the presence of water reducing the pro-

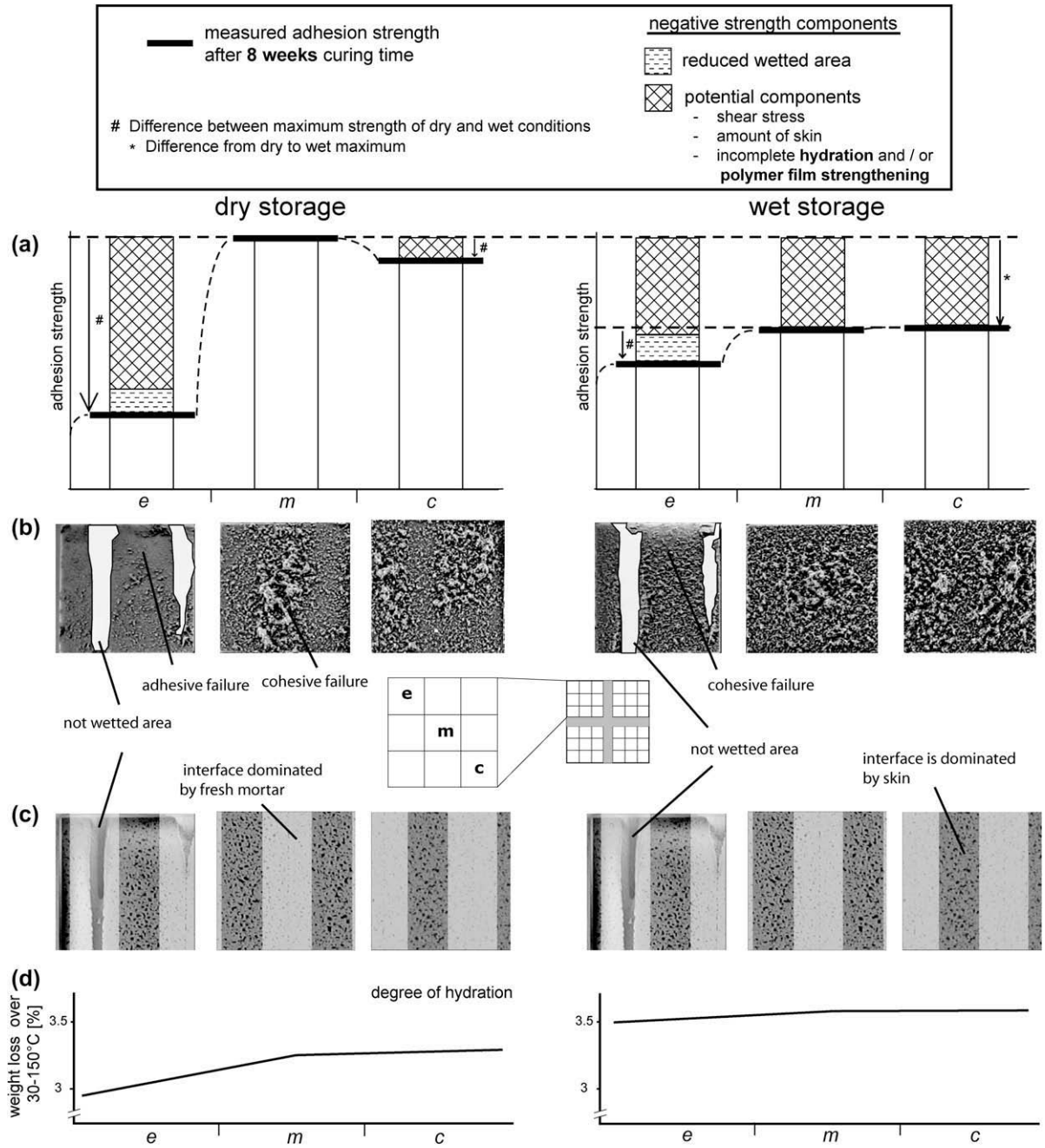

Fig. 15. Mechanical properties as a function of positions (*e* = edge, *m* = middle, *c* = core) and storage conditions (dry and wet storage). (a) The adhesion strengths were obtained from pull-out tests after 8 weeks. Position *m* (dry) is considered to be ideal and the difference to this value at other positions is given by the negative strength components. (b) Mosaic backsides (*e*, *m*, *c*) after pull-out test after 8 weeks of dry and wet storage, respectively. (c) Positions *e*, *m*, *c* seen through glass plate (see also Fig. 10). (d) Degree of hydration, gained by TGA measurements after 4 weeks (only positions corresponding to *e* and *c* were measured, see also Fig. 12).

gress in polymer film formation and therefore the polymers' strength. This may partly explain the difference in adhesion strength between dry and wet stored samples (see ∗ in Fig. 15).

As the thermogravimetric analyses have shown (Fig. 12), the difference in degree of hydration between core and rim is low (less than 5%) for the wet storage. Even though the difference between core and rim is higher for the dry stored samples (10%), the difference is rather low by comparison to the difference in adhesion strength between core and rim. For this reason, we argue that additional mechanisms must account for the differences, e.g. the degree of polymer strengthening.

4.2.4. Shear stress

The shrinkage of mortar (drying, hydration) and substrate (drying) leads to differential movement. This difference is highest at the interface between tile and mortar due to the highest material contrast. This leads to shear stresses, which are rising gradually from centre to rim of a tile [24]. At the time the shear stresses exceed a critical value, micro-cracking occurs. Additionally, one has to keep in mind that significant shrinkage over the entire assembly occurs between the 6th and 10th week. The coincidence of the timing of: (i) the enhanced shrinkage, (ii) the decrease in adhesion strength and (iii) the delamination for dry storage point to a con-

tinuous excess of the shear stresses associated with progressive adhesion failure. Enclosed with the drying-induced continuous embrittlement of the mortar [22], micro-cracking results. In that time range, a decrease in adhesion strength is missing for the wet storage although shrinkage and delamination occur. At the present stage, we can only speculate on the origin of this difference to the dry storage. As Jenni et al. [15] demonstrated, nucleation of hydration products can occur in cavities. Hence, the potential formation of shrinkage-induced cracks might be healed with the hydrates preserving a constant rise in adhesion strength.

5. Conclusions

Using an application setup without grouts, environmental situations for extreme interaction between mortar and air and water, respectively, were provoked for two series of single-applied large-sized tiles. For both storage conditions, different evolutions of adhesion strength were shown for: (i) the entire sample and for (ii) single positions. In the case of dry storage, an increase of the adhesion strength correlates with enhanced hydration and polymer film formation. For the wet stored samples, the long-lasting presence of water still increases the degree of hydration, but retards the strengthening of the polymers films. Reduced adhesion strengths are observed on positions where the fracture pattern mainly is characterized by adhesion failure. This observation indicates that the tile-mortar interface reflects the weakest domain in the entire assembly. The adhesion strength is reduced by: (i) shear stresses owing to drying and hydration shrinkage, (ii) incomplete wetting and (iii) the occurrence of a mortar skin at the tile-mortar interface. It is therefore the combination of all these effects, which controls the physical behaviour of the bulk assembly.

Lowest adhesion strength was registered at the edge position, which correlates with typical damage locations on the construction site. Edge positions are critical because constant weathering in outdoor applications enhances the risk of damage. At these sites, water intrudes first into the system as shown by water immersion of glass plate samples. In order to prevent failures on entire claddings at the edge positions of the tiles, the adhesion strength at these sites must be enhanced. This goal could be achieved by polymer modification, which counteracts early drying and resulting low degree of hydration by complementary early film formation. It could also be achieved by enhanced wetting at the tile-mortar interface. Further, the adhesion can be improved by reducing the skin at the interface. This reduction can be reached by shortening the time interval between application of the mortar and the inlaying of the tile. Especially for arid climatic conditions, it is crucial to keep the open time low, because such climatic conditions accelerate the skin formation [19].

Another problem is the use of porcelain tiles, because the vitreous surface additionally degrades the adhesion at the tile-mortar interface. In order to reduce shear stresses, which are highest at the mentioned edge position, the use of small-sized tiles would favour a reduction in shear stresses. Unfortunately, this mechanical advantage opposes the design-driven market trends towards large-sized tiles.

Acknowledgements

Financial support by the Swiss Commission for Technology and Innovation (CTI) is gratefully acknowledged (CTI Project No. 8605.1 EPRP-IW). The authors would like to thank Hanspeter Waser (Elotex) for support of experiments and Josef Kaufmann, Frank Winnefeld and Sandy Harzer (Empa) for discussions.

References

[1] Silvestre JD, de Brito J. Ceramic tiling inspection system. Constr Build Mater 2009;23:653–68.
[2] Mansur AAP, Nascimento OL, Mansur HS. Data collection of five years of exterior facade pathologies in Brazil. In: IX world congress on ceramic tile quality. Castellon (Spain): Logui Impresión; 2006. p. PBB107–20.
[3] Chew MYL. Factors affecting ceramic tile adhesion for external cladding. Constr Build Mater 1999;13:293–6.
[4] Yiu CY, Ho DCW, Lo SM. Weathering effects on external wall tiling systems. Constr Build Mater 2007;21:594–600.
[5] Felixberger J. Einflussfaktoren auf den Haftverbund Untergrund – Fliese – keramischer Belag. In: Plank J, Stephan D, editors. 5. Tagung Bauchemie München: GDCh-Fachgruppe Bauchemie; 2003. p. 47–53.
[6] Bijen J, Schlangen E, Salet T. Modelling of effects of shrinkage on the performance of adhesives. In: Ohama Y, Puterman M, editors. 2nd International RILEM symposium on adhesion between polymers and concrete. Dresden (Germany): RILEM Publications; 1999. p. 299–310.
[7] Sanchez E, Ibanez MJ, Garcia-Ten J, Quereda MF, Hutchings IM, Xu YM. Porcelain tile microstructure: implications for polished tile properties. J Eur Ceram Soc 2006;26:2533–40.
[8] Carty WM, Senapati U. Porcelain – raw materials, processing, phase evolution, and mechanical behavior. J Am Ceram Soc 1998;81:3–20.
[9] Almeida AEFD, Sichieri EP. Experimental study on polymer-modified mortars with silica fume applied to fix porcelain tile. Build Environ 2007;42:2645–50.
[10] Mansur AAP, Santos DB, Mansur HS. A microstructural approach to adherence mechanism of poly (vinyl alcohol) modified cement systems to ceramic tiles. Cem Concr Res 2007;37:270–82.
[11] Ohama Y. Book handbook of polymer-modified concrete and mortars, properties and process technology. Park Ridge, New Jersey (USA): Noyes Publications; 1995.
[12] Schulze J. Influence of water–cement ratio and cement content on the properties of polymer-modified mortars. Cem Concr Res 1999;29:909–15.
[13] Jenni A, Herwegh M, Zurbriggen R, Aberle T, Holzer L. Quantitative microstructure analysis of polymer-modified mortars. J Microsc – Oxford 2003;212:186–96.
[14] Dimmig-Osburg A, Pietsch I, Pietsch J. Polymer additives and their influence on the cement microstructure in the early stages of hardening. ZKG Int 2006;59:72–83.
[15] Jenni A, Zurbriggen R, Holzer L, Herwegh M. Changes in microstructures and physical properties of polymer-modified mortars during wet storage. Cem Concr Res 2006;36:79–90.
[16] De Gasparo A. Fractionation behavior of organic additives and resulting microstructural evolution of mixed-binder based self-leveling flooring compounds. PhD thesis. Bern: Bern University; 2006.
[17] Jenni A, Holzer L, Zurbriggen R, Herwegh M. Influence of polymers on microstructure and adhesive strength of cementitious tile adhesive mortars. Cem Concr Res 2005;35:35–50.
[18] De Gasparo A, Herwegh M, Zurbriggen R, Scrivener K. Quantitative distribution patterns of additives in self-leveling flooring compounds (underlayments) as function of application, formulation and climatic conditions. Cem Concr Res 2009;39:313–23.
[19] Oberste-Padtberg R, Sieksmeier J. Factors influencing the open time of building mortars. In: Leopolder F, editor. Drymix mortar yearbook 2007. Nürnberg (Germany): Drymix.info; 2007. p. 44–9.
[20] Winnefeld F, Kaufmann J, Harzer S, Herwegh M, Wetzel A, Zurbriggen R. Hydration and moisture gradients of tile adhesives. In: Fischer H-B, Bode K-A, editors. 17. Internationale Baustofftagung ibausil. Weimar (Germany): FA Finger-Institut für Baustoffkunde; 2009. p. 967–72.
[21] Bentz DP, Haecker CJ, Peltz MA, Snyder KA. X-ray absorption studies of drying of cementitious tile adhesive mortars. Cem Concr Compos 2008;30:361–73.
[22] Routh AF, Russel BR. A process model for latex film formation: limiting regimes for individual driving forces. American Chemical Society; 1999.
[23] Du Chesne A, Bojkova A, Gapinski J, Seip D, Fischer P. Film formation and redispersion of waterborne latex coatings. J Colloid Interf Sci 2000;224:91–8.
[24] Herwegh M, Mettier R, Zurbriggen R, Wetzel A, Winnefeld F, Kaufmann J. Critical stress concentrations in tile adhesive mortars: a numerical modelling approach. In: Fischer H-B, Bode K-A, editors. 17. Internationale Baustofftagung ibausil. Weimar (Germany): FA Finger-Institut für Baustoffkunde; 2009. p. 137–41.